Suggested overall title: Preliminary analytical validation of DEM codes

1. Introduction

Prior to embarking on the round robin test exercise, participants may find it useful to confirm that the DEM codes they are using can capture some simple, well constrained problems. In each case these are problems for which an analytical solution can be found, so that any uncertainty associated with experimental measurements is avoided. This selection of verification / validation problems considers single particle behaviour and multiple particle behaviour. Reference to appropriate key references is made in each case and some input parameters are suggested. The selection of verification problems is restricted to spherical particles.

2. Single particle interaction: Ball Rolling Down a Horizontal Plane

2.1 Problem Description

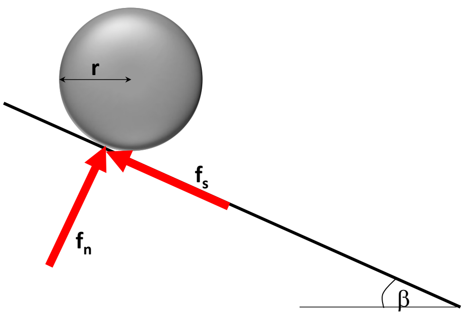

Figure 2.1: Schematic of ball rolling down an inclined plane.

This problem is considered in Ke & Bray (1995), O'Sullivan & Bray (2003), Huang et al. (2014) and Artigaut (2019). It is applicable to both 2D and 3D DEM codes. Ke & Bray (1995) provide the necessary information to apply this problem to a 2D DEM code. Considering the 3D case, referring to Figure 2.1, consider the case of a ball on an inclined plane. The ball should be just in contact with the inclined plane. The ball radius is r, the ball mass is M, the inclination of the plane is β, and the angle of friction between the ball and the inclined plane is ϕ. The ball will either roll or slide down the plane, depending on the value of ϕ relative to β.

Ke & Bray (1995) give the limiting friction angle between sliding and rolling for a disk rolling down the plane as:

$$\phi_L = tan^{-1}\left(sin\left(\frac{\beta}{3}\right)\right) \quad (2.1)$$

However in the case of a sphere this needs to be re-calculated.

There are two cases to consider, as follows:

(i) In the case of sliding, i.e. where $\phi < \phi_L$

$$\boldsymbol{f}_n = M\boldsymbol{g}cos\beta \quad (2.2)$$

$$\boldsymbol{f}_s = M\boldsymbol{g}cos\beta tan\phi \quad (2.3)$$

where $\boldsymbol{f}_n$ is the normal component of the contact force between the ball and the inclined plane, $\boldsymbol{f}_s$ is the shear or tangential component of the contact force, and $\boldsymbol{g}$ is acceleration due to gravity.

The particle translational acceleration is then given by

$$\ddot{\boldsymbol{a}} = \boldsymbol{g}(sin\beta - cos\beta tan\phi) \qquad (2.4)$$

As the moment of inertia of the sphere is $I = \frac{2}{5}Mr^2$, the rotational acceleration ($\ddot{\boldsymbol{\theta}}$) and velocity ($\dot{\boldsymbol{\theta}}$) and accumulated rotation ($\boldsymbol{\theta}$) are given by $\boldsymbol{f}_s/\, I$:

$$\ddot{\boldsymbol{\theta}} = \frac{5}{2}\frac{gcos\beta tan\phi}{r} \ (2.5)$$

$$\dot{\boldsymbol{\theta}} = \frac{5}{2}\frac{gcos\beta tan\phi}{r} t \ (2.6)$$

$$\boldsymbol{\theta} = \frac{5}{4}\frac{gcos\beta tan\phi}{r} t^2 \ (2.7)$$

(ii) In the case of rolling, i.e. where $\phi > \phi_L$

In the case of pure rolling there is no sliding and so at the point of contact the linear and rotational velocities must equal so that

$$\dot{\boldsymbol{\theta}} r = -\boldsymbol{v} \ (2.8)$$

Where the linear velocity is given by

$$\boldsymbol{v} = \boldsymbol{g}(sin\beta - cos\beta tan\phi)t \ (2.9)$$

Thus the limiting friction, ϕ_L, delineating sliding from rolling, is that where

$$tan\phi_L = \frac{2}{7} tan\beta \ (2.10)$$

For β=45 degrees, this gives ϕ_L=15.95 degrees.

2.2 Suggested input parameters

This simulation can be achieved either by inputting the coordinates of the inclined plane or by applying an inclined gravitational body force.

In their 2D disk simulations Ke and Bray (1995)used a linear contact model with a normal spring stiffness of 1e10 N/m, and a shear stiffness of 1e9 N/m, disk radius of 1 m (particle density not specified).

In 3D Artigaut (2019) used LIGGGHTS with a Hertz-Mindlin contact model and the parameters listed in Table 1.

Table 1: Suggested input parameters for verification of ball rolling down an inclined plane with

Parameter	Value	Unit
Particle diameter (=2r)	1 x 10^{-3}	m
Particle density	2650	Kg/m^3
Particle Young's modulus, E	6 x 10^{10}	N/m
Particle Poisson's ratio	0.20	
Particle coefficient of restitution	0.051	

2.3 Expected results

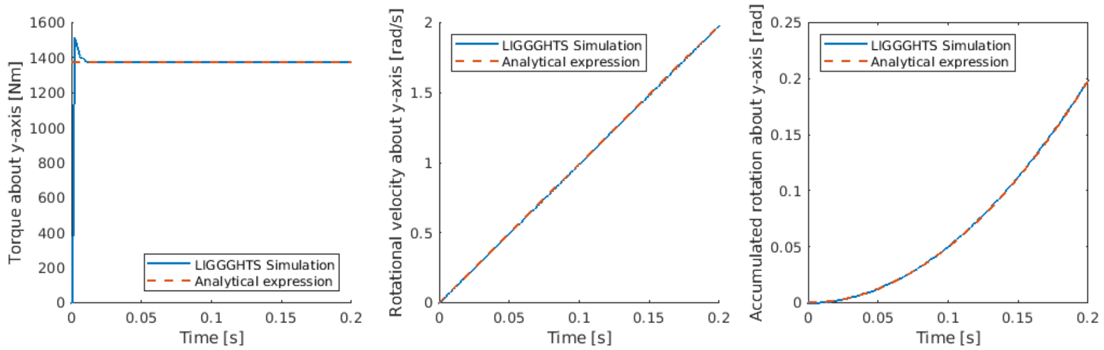

Figure 2.2 Expected simulation results for case of β=45 degrees, (a) Torque versus time, (b) Rotational velocity , $\dot{\theta}$, versus time, (c) Accumulated rotation, θ, versus time. (Artigaut, 2019)

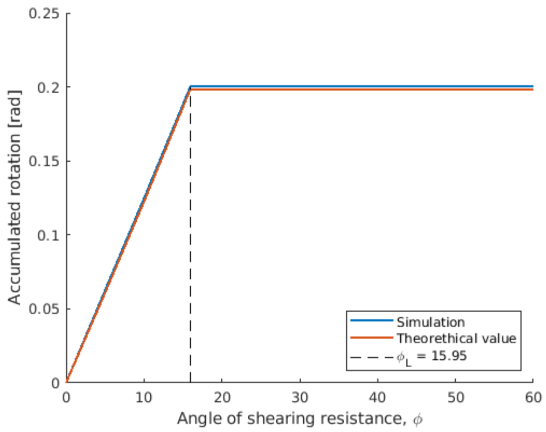

Figure 2.3 Expected simulation results for case of β=45 degrees, accumulated rotation after 0.2s. (Artigaut, 2019)

3 3D case of an assembly of uniform spheres with a face-centred-cubic packing

3.1 Description of problem

As identified in the documentation of the DEM code Trubal (Cundall and Strack, 1979), and in the user manuals for PFC (e.g. Itasca Consulting Group, 2007), simulation of drained triaxial and true-triaxial compression tests on samples of uniform spheres on a lattice packing are useful to verify that a DEM code can capture the response of a system of particles. Simulations of these systems can, for example, be useful to identify whether the time step used in simulations is appropriate (Otsubo, O'Sullivan and Shire, 2017). Representative packing images are provided in Figure 3.1.

Consideration of these systems is useful as the symmetry of the system enables analytical expressions for the strength in triaxial expression to be developed. For example, the response of an assembly of face-centred-cubic spheres was considered by Rowe (1962) and Thornton (1979). From Thornton (1979) the stress ratio at failure for this system subject to triaxial compression is given by

$$\frac{\sigma_1}{\sigma_3} = \frac{2(1+\mu)}{1-\mu}$$

where σ_1, is the major principal stress, σ_3 is the minor principal stress, and $\mu = \tan\phi$ is the coefficient of friction between the spheres.

This expression can be applied whether the simulations are run using periodic boundaries or rigid wall boundaries. Where rigid wall boundaries are used attention should be paid to the simulation size; it is important to achieve a representative element volume.

To replicate the analytical expressions particle rotations should be inhibited to simulate an "irrotational" condition.

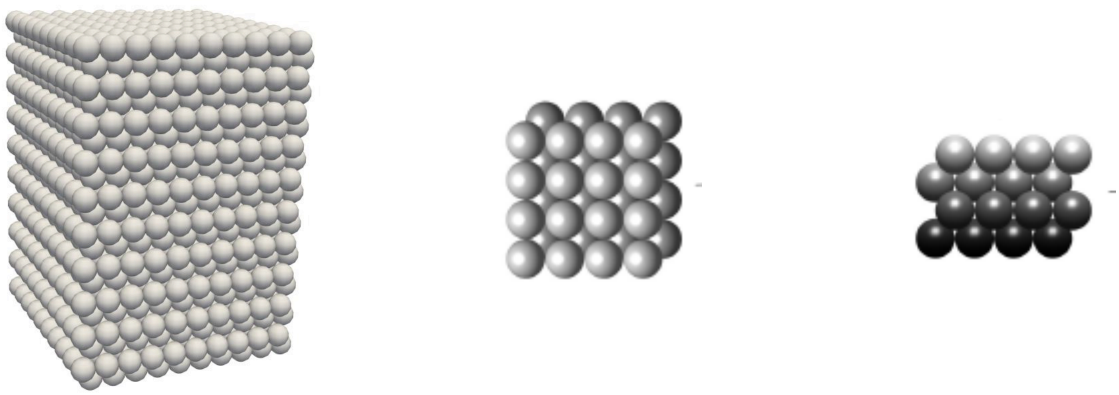

(a) Perspective view (2000 spheres) **(b) Plan view of subset of packing (xy plane)** **(c) Plan view of subset of packing (xz plane)**

Figure 3.1 Visualization of face-centred-cubic assembly of discs for simulation using periodic cell system (Huang, 2014)

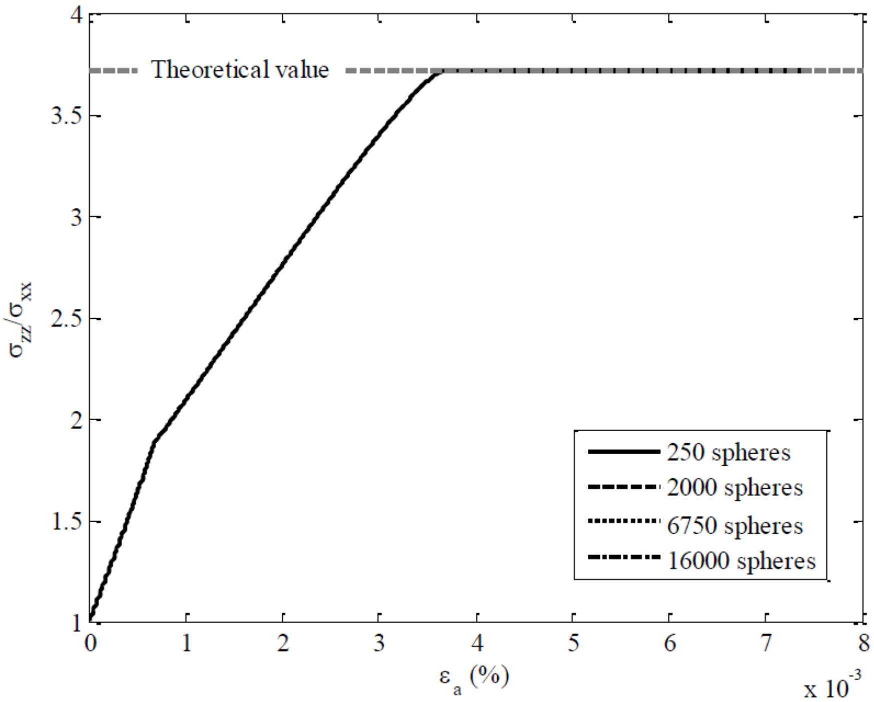

Figure 3.2 : Variation in stress ratio ($\frac{\sigma_1}{\sigma_3} = \frac{\sigma_{zz}}{\sigma_{xx}}$)with axial strain for periodic-cell simulation of triaxial compression of a face-centred-cubic assembly of uniform spheres: DEM code LAMMPS (Huang, 2014) ()

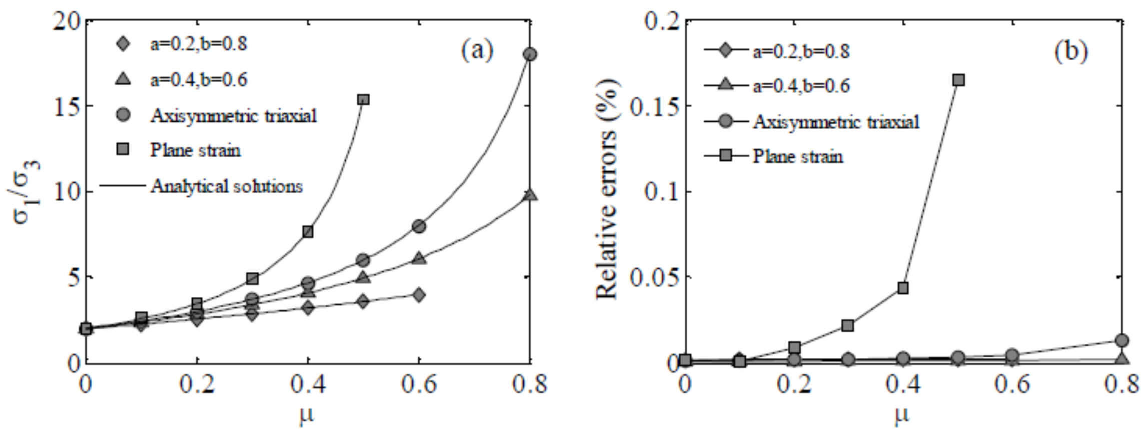

Figure 3.4 : Variation in peak stress ratio with interparticle friction coefficient for periodic-cell simulation of triaxial compression of a face-centred-cubic assembly of uniform spheres. Comparison with the analytical expressions provided by Thornton (1979): DEM code LAMMPS (Huang, 2014)

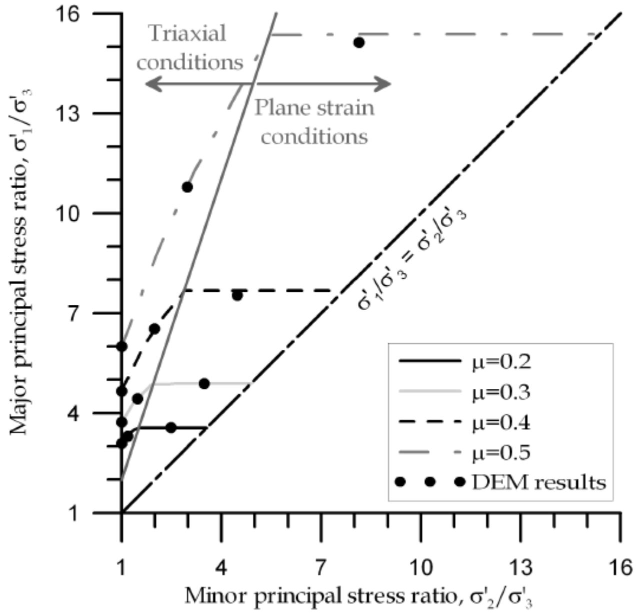

Figure 3.3 : Variation in peak stress ratio with interparticle friction coefficient for periodic-cell simulation of true-triaxial compression of a face-centred-cubic assembly of 2,600 uniform spheres. Comparison with the analytical expressions provided by Thornton (1979): DEM code modified Trubal (Barreto Gonzalez, 2009)

3.2 Suggested input parameters

- Huang (2014) considered samples with 250, 2,500, 6,750 and 16,000 spherical particles. In all cases the particle diameter was 0.01m, the density was 2,670 kg/m^3, the particle shear modulus was G=1x10^{12} Pa, the Poisson's ratio was ν= 0.22 and the coefficient of friction was 0.2. A vertical strain rate of 5 x 10^{-3} m/s was adopted.
- Knight (2014) used periodic boundaries, a sphere diameter of 2 m, a particle density of 1 x 10^4 kg/m^3. He used a simplified Hertz-Mindlin contact model with a Young's modulus of 7 x 10^{10}Jm^{-3}, a shear modulus of 2.92 x 10^{10}Jm^{-3} and a Poisson's ratio of 0.20. Knight used 512 spheres, each layer comprised 8 x 8 particles and there were 8 layers.
- Barreto (2009) used periodic boundaries, a sphere diameter of 0.75 mm, a particle density varying between 2.56x10^{-8} kg/mm^3 and 2.56x10^{-4} kg/mm^3. He used a simplified Hertz-Mindlin contact model with a shear modulus of 28,688 N/mm^2 and a Poisson's ratio of 0.20-0.5. Barreto used 2600 spheres, each layer comprised 10 x 10 particles and there were 26 layers.
- Otsubo (2016) used lateral periodic boundaries and rigid walls at the top and bottom of his samples. He used a sphere radius of 2.54 x 10^{-3} m and a particle density of 2,230 kg/m^3. He used a simplified Hertz-Mindlin contact model with a shear modulus of 25.0 GPa and a Poisson's ratio of 0.2. His strain rate was 0.001s^{-1} and he used a viscous damping parameter of 0.1. His sample compressed 200 layers of 4 x 4 (16 spheres).
- O'Donovan (2013) considered the experiment by Rowe (1962) and the triaxial test simulation configuration described in the original Trubal report (Cundall and Strack, 1979). He had rigid walls at the top and bottom and he applied specific forces to the external particles to achieve his target confining pressure. His particle properties were in line with Rowe's experiments. O'Donovan adopted a sphere radius of 20 mm and a particle density of 2000 g/mm^3. He used

a modified Hertz-Mindlin contact model with a shear modulus of 77.82 GPa, a Poisson's ratio of 0.285 and a coefficient of friction of 0.1228.

Acknowledgements

Apart from the contributions of former students cited, discussions with Dr. Adnan Sufian, University of Queensland and Dr. Kevin Hanley, University of Edinburgh, underlie many of the details in this discussion. Tara Sassel and Deyun Liu, doctoral students at Imperial College London, kindly proof-read this document.

References

Artigaut, M. (2019) *Simulation of seepage in sand using coupled CFD-DEM*. Imperial College London.

Barreto Gonzalez, D. (2009) *Numerical and expeirmental investigation into the behaviour of granular materials under generalised stress states*. University of London.

Cundall, P. A. and Strack, O. D. L. (1979) 'The distinct element method as a tool for research in granular media', *Report to the National Science Foundation*.

Huang, X. (2014) *Exploring critical-state behaviour using DEM*. The University of Hong Kong and Imperial College London.

Huang, X. *et al.* (2014) 'Exploring the influence of interparticle friction on critical state behaviour using DEM', *International Journal for Numerical and Analytical Methods in Geomechanics*, 38(12). doi: 10.1002/nag.2259.

Itasca Consulting Group (2007) *PFC3D Version 4.0 User Manual*. Minneapolis, MN, USA.: Itasca Consulting Group.

Ke, T. and Bray, J. (1995) 'Modeling of Particulate Media Using Discontinuous Deformation Analysis', *Journal of Engineering Mechanics*, 121(11), pp. 1234–1243. doi: 10.1061/(ASCE)0733-9399(1995)121:11(1234).

Knight, C. S. (2014) *A validation of DEM codes by comparison with the analytical solution for the peak shear strength at failure of a regular assembly of smooth spheres*. Imperial College London.

O'Donovan, J. (2013) *Micromechanics of Wave Propagation through Granular Material, PhD thesis.* Imperial College London.

O'Sullivan, C. and Bray, J. D. (2003) 'Modified Shear Spring Formulation for Discontinuous Deformation Analysis of Particulate Media', *Journal of Engineering Mechanics*, 129(7), p. 830. doi: 10.1061/(ASCE)0733-9399(2003)129:7(830).

Otsubo, M. (2016) *Particle scale analysis of soil stiffness and elastic wave propagation*. Imperial College London.

Otsubo, M., O'Sullivan, C. and Shire, T. (2017) 'Empirical assessment of the critical time increment in explicit particulate discrete element method simulations', *Computers and Geotechnics*, 86. doi: 10.1016/j.compgeo.2016.12.022.

Rowe, P. (1962) 'The stress-dilatancy relation for static equilibrium of an assembly of particles in contact', *Proceedings of the Royal Society of Science. Series A, Mathematical and Physical Sciences*, 269(1339), pp. 500–527.

Thornton, C. (1979) 'The conditions for failure of a face-centered cubic array of uniform rigid spheres', *Géotechnique*, 29(4), pp. 441–459. doi: 10.1680/geot.1979.29.4.441.